Published in final edited form as:
J Comb Chem. 2010 November 8; 12(6): 836–843. doi:10.1021/cc100091h.

Design, Synthesis and In Vitro Evaluation of Potential West Nile Virus Protease Inhibitors Based on the 1-Oxo-1, 2, 3, 4-tetrahydroisoquinoline and 1-Oxo-1, 2-dihydroisoquinoline Scaffolds

Dengfeng Dou[#], **Prasanth Viwanathan**[+], **Yi Li**[#], **Guijia He**[#], **Kevin R. Alliston**[#], **Gerald H. Lushington**[@], **Joshua D. Brown-Clay**[+], **R. Padmanabhan**[+], and **William C. Groutas**[#,*]

[#] Department of Chemistry, Wichita State University, Wichita, Kansas 67260

[+] Department of Microbiology and Immunology, Georgetown University Medical Center, Washington, DC 20057

[@] Molecular Graphics and Modeling Laboratory, The University of Kansas, Lawrence, KS 66045

Abstract

The 1-Oxo-1, 2, 3, 4-tetrahydroisoquinoline and 1-Oxo-1, 2-dihydroisoquinoline scaffolds were utilized in the design and solution phase synthesis of focused libraries of compounds for screening against West Nile Virus (WNV) protease. Exploratory studies have lead to the identification of a WNV protease inhibitor (a 1-oxo-1, 2-dihydroisoquinoline-based derivative, ***12j***) which could potentially serve as a launching pad for a hit-to-lead optimization campaign. The identified hit was devoid of any inhibitory activity toward a panel of mammalian serine proteases.

Introduction

Proteases account for ~2% of the genes in humans and infectious organisms and are involved in the regulation of a multitude of essential physiological processes. A wide range of human diseases are associated with the aberrant activity of proteases (1–2). Furthermore, many proteases are essential to the survival of bacterial, viral, parasitic, and fungal pathogens.

West Nile virus (WNV), a member of the Flavivirus genus of the *Flaviviridae* family, has emerged as an important mosquito-borne viral pathogen (3). No effective vaccines or antiviral agents are currently available for the prevention or treatment of WNV (4). WNV is a small, enveloped virus with a single-stranded, positive sense 11-kb RNA genome, which encodes a polyprotein precursor. Co-and post-translational cleavage of the polyprotein produces three structural (C, prM, and E) and seven nonstructural (NS1, NS2A, NS2B, NS3, NS4A, NS4B, and NS5) proteins by a concerted action of a host signal peptidase and the trypsin-like viral serine protease. The viral protease encoded within NS3 in conjunction with the NS2B cofactor cleaves at NS2A-NS2B, NS2B-NS3, NS3-NS4A, and 4B-NS5 sites, as well as some internal sites within C, NS3 and NS4A. Cleavage at these sites is essential for viral replication. Thus, WNV NS2B/NS3 protease has emerged as an important target for the design and development of novel therapeutics against West Nile virus (5).

[*]author to whom correspondence should be addressed: Department of Chemistry, Wichita State University, Wichita, KS 67260, Tel. (316) 978 7374; Fax: (316) 978 3431, bill.groutas@wichita.edu.

Flavivirus NS2B is an endoplasmic membrane-associated hydrophobic protein of 130 amino acid residues (6). Active protease consists of a heterodimeric complex of NS2B and NS3. The amino terminal part of NS3 that contains the serine protease catalytic triad is sufficient for interaction with NS2B and activation of the protease domain. The carboxy terminal portion of NS3 contains ATPase, RNA helicase and 5′ RNA triphosphatase activities and performs other functions in the virus life cycle such as viral replication and 5′ capping (7–8).

The viral serine protease cofactor NS2B protein consists of three hydrophobic regions flanking a conserved hydrophilic domain of 45 amino acid residues. For the function of the viral protease in infected host cells, the hydrophobic regions of NS2B as well as the hydrophilic domain are required (7), however, the latter domain alone is sufficient for the interaction with the NS3 protease domain and for in vitro protease activity in cleaving the polyprotein substrate at specific sites. These sites contain two basic amino acid residues at the P1 and P2 positions (9) followed by a residue with a short side chain (Ala, Ser, or Gly) at the P1′ position (6,10–12).

The substrate specificity of WNV protease has been probed using peptidyl substrates and inhibitors (4(b), 12–13) and X-ray crystallography. The active site of WNV NS2B/NS3 protease, consisting of His51, Asp75 and Ser135, is located at the interface of the N- and C-terminal lobes and prefers a dibasic motif at P1-P2 (14). X-ray crystal structures of WNV NS2B-NS3pro complexed to aprotinin (Bowman Pancreatic Trypsin Inhibitor (BPTI) (15) and Bz-Nle-Lys-Arg-Arg-CHO (16), respectively, have been reported. Inhibitors of WNV protease containing a highly charged peptidyl or non-peptidyl recognition component reflecting the substrate specificity of the protease include peptidyl aldehydes (17), D-Arg-based peptides (18), and guanidine-based compounds (19). Other low molecular weight inhibitors of the protease include pyrazoline (20) and sultam thiourea (21) derivatives and others (22). There is currently a need for low molecular weight non-peptidyl agents that exhibit superior potency, selectivity and drug-like characteristics. We report herein the results of preliminary studies related to the use of 1-oxo-1, 2, 3, 4-tetrahydroisoquinoline and 1-oxo-1, 2-dihydroisoquinoline-based derivatives as potential inhibitors of WNV protease.

Results and Discussion

Inhibitor design

The biochemical rationale underlying the use of the 1-oxo-1, 2, 3, 4-tetrahydroisoquinoline scaffold in the design of serine protease inhibitors rested on the following considerations: (a) previous studies related to the steric course and specificity of α-chymotrypsin-catalyzed reactions have shown that D-1-oxo-1, 2, 3, 4-tetrahydroisoquinoline 3-carboxymethyl ester (Figure 1(a)) behaves as a relatively efficient substrate of the enzyme, indicating that the heterocyclic scaffold is capable of binding productively to the active site of the enzyme (23); (b) WNV NS2B-NS3pro is a trypsin-like serine protease with a prototypical catalytic triad and an active site that is located at the interface of the N- and C-terminal lobes. We reasoned that an entity such as (I) (Figure 1) that embodied a recognition element (1-oxo-1, 2, 3, 4-tetrahydroisoquinoline scaffold) and a suitably-positioned serine trap may function as a non-peptidyl transition state inhibitor of the viral protease (Figure 1(b)) (24). Of particular interest were the α-ketoamide derivatives (structure (I), Z = CONHR), since judicious changes in the nature of the R group could potentially lead to the exploitation of additional favorable binding interactions.

Synthesis

We initially set out to prepare aldehyde ***3*** from compound ***2*** (Scheme 1) since it would serve as a suitable intermediate for synthesizing the desired inhibitors. Thus, when compound ***2*** was treated with DIBAL (25) only the starting material was recovered. An alternative method for making ***3***, also unsuccessful, involved the treatment of ***2*** with iodotrimethylsilane in methylene chloride to give the corresponding trimethylsilyl ether ($RCOOSi(CH_3)_3$) which was then treated with DIBAL, as described in the literature (26). Lithium aluminum hydride reduction of ester ***2*** in the presence of diethylamine (27) failed to give **3** and gave instead the corresponding alcohol. A second approach toward the synthesis of ***3*** was pursued which involved reduction of ***2*** ($LiBH_4$/THF) to give alcohol ***4*** followed by treatment with pyridinium chlorochromate in methylene chloride (28). NMR analysis of the complex reaction mixture showed the absence of any aldehyde, despite complete consumption of the starting alcohol. Swern oxidation of **4** yielded a white solid the structure of which was established by X-ray crystallography to be that of compound ***5***. It is evident that aldehyde ***3*** is formed which then dimerizes to ***5*** under the reaction conditions. Further attempts to generate variants of (I), such as the direct formation of (I) with Z = heterocycle (29), were also unsuccessful and necessitated a change in strategy that entailed the solution-phase generation of a library of compounds based on the 1-oxo-1, 2, 3, 4-tetrahydroisoquinoline scaffold that could potentially function as reversible competitive inhibitors of the enzyme. Thus, the synthesis of compounds ***7*****(a–f)** proceeded uneventfully when aliphatic amines were used (Scheme 2 (a)), however, an alternative route was utilized in the synthesis of compounds ***7(g–j)*** derived from aromatic amines (Scheme 2 (b)). The unusually low yields are probably due to steric effects, the use of non-optimized conditions, and loss of sample during the purification of the compounds. A fairly diverse set of amine inputs (Table 1) was utilized for optimal space exploration. With the exception of compound ***7g*** (~25% inhibition at 50 μM inhibitor concentration), the rest of the compounds were devoid of any inhibitory activity against WNV protease, suggesting that these compounds do not engage in multiple binding interactions with the target enzyme. This series of compounds was inactive against a representative panel of serine proteases, including bovine α-chymotrypsin, human neutrophil elastase, cathepsin G, and human skin chymase (30). Intriguingly, compounds ***7f*** and ***7h*** were found to inhibit bovine trypsin (42% and 22% inhibition, respectively, at a 50 μM inhibitor concentration).

The exploratory studies cited above suggested that the non-planar component in (I) may be inimical to binding, consequently a focused library of compounds (***10c, 10f, 12a–c, 12f, 12j***) was generated based on the 1-oxo-1, 2-dihydroisoquinoline scaffold and its bromo variant using Scheme 3. Screening of these libraries resulted in the identification of a hit (compound ***12j***) that was found to be a fair inhibitor of WNV protease (IC_{50} 30 μM). A plausible mode of binding of energy-minimized compound ***12j*** to the active site of the enzyme is illustrated in Figure 2(a–b). The aromatic portion of the bromisoquinoline moiety forms a π-stacking interaction with Y161 and engages in end-on hydrophobic interactions with Y150. The amide on the bromoisoquinoline group hydrogen bonds with the hydroxyl side chain of the catalytic S135, namely, the carbonyl oxygen on bromoisoquinoline serves as a hydrogen acceptor from the S135 proton and the amide proton serve as hydrogen bond donor to the S135 hydroxyl oxygen. The amide proton on the linker between the bromoisoquinoline and the (m-phenoxy) phenyl is predicted to hydrogen bond with the backbone carbonyl of G151. The first aromatic ring in the (m-phenoxy)phenyl group is solvent exposed and is not predicted to participate in any significant favorable interactions. However, the second aromatic ring interacts with the side chain of V72, with the mildly hydrophobic β carbons of His51 and D75, and has an end-on hydrophobic interaction with W50. Although the aromatic portion of the bromoisoquinoline moiety engages in π-stacking interactions and fits well within a very small cavity, it might be possible to improve the affinity for this cavity by

noting that the end of the ring points toward highly polar species, such as the D129 side chain and the Y130 backbone. Furthermore, the first aromatic ring in the (m-phenoxy)phenyl component serves as a semi rigid spacer of ideal length for fostering the favorable interactions associated with the bromoisoquinoline ring and on the second aromatic ring in the (m-phenoxy)phenyl component. Consequently, exploring other groups that maintain the same spacer distance and orientation may provide additional opportunities for affinity enhancement.

In summary, exploratory studies utilizing the 1-oxo-1, 2-dihydroisoquinoline scaffold have led to the identification of an inhibitor of WNV protease suitable for further exploration.

Experimental Section

General

The ^{1}H NMR spectra were recorded on a Varian XL-300 or XL-400 NMR spectrometer. A Gemini EM microplate spectrofluorometer (Molecular Devices Corporation, Sunnyvale, CA) was used in the enzyme assays and inhibition studies. Melting points were determined on a Mel-Temp apparatus and are uncorrected. Reagents and solvents were purchased from various chemical suppliers (Aldrich, Acros Organics, TCI America, and Bachem). Silica gel (230–450 mesh) used for flash chromatography was purchased from Sorbent Technologies, Atlanta, GA. Thin layer chromatography was performed using Analtech silica gel plates. The TLC plates were visualized using iodine and/or UV light. WNV protease was expressed in *E. coli* as described for Dengue virus-2 protease (12) and was purified as previously described (14). Boc-Gly-Lys-Arg-AMC was purchased from Bachem. The purity of all compounds was established by TLC. HPLC analyses were performed on a Varian Prostar 320 monitored at 280 nm using a C18 Luna2 250 × 4.6 mm column with an isocratic 45% acetonitrile and 55% aqueous solution containing 5% methanol and 0.1% formic acid.

Synthesis

(DL)Methyl 2-isocyanato-3-phenylpropanoate 1—DL-phenylalanine methyl ester hydrochloride (13.6 g; 63 mmol) was placed in a round bottom flask and pumped under high vacuum overnight. Dioxane (150 mL) was then added, followed by trichloromethyl chloroformate (10.5 mL; 88.5 mmol). The resulting mixture was refluxed gently overnight. The solvent was removed and the residue was distilled under reduced pressure to give the corresponding isocyanate ***1*** as a colorless oil (12.9 g, 99% yield). ^{1}H NMR ($CDCl_3$) δ 3.03 (dd, J = 13.7, 5.0 Hz, 1H), 3.16 (dd, J = 13.7, 8.2 Hz, 1H), 3.81(s, 3H), 4.02–4.10 (m, 1H), 7.18–7.38 (m, 5H).

(DL)Methyl 1-oxo-1,2,3,4-tetrahydroisoquinoline-3-carboxylate 2—To a solution of compound ***1*** (12.9 g; 63 mmol) in dry methylene chloride (120 mL) was added $AlCl_3$ (16.8 g; 126 mmol) in small portions and the resulting mixture was refluxed for 2 h. The reaction mixture was allowed to cool to room temperature and then placed in an ice-water bath. Water (100 mL) was slowly added and the mixture was stirred for 30 minutes. The two layers were separated and the organic layer was dried over anhydrous sodium sulfate. Removal of the solvent left a crude product which was purified by flash chromatography (silica gel/ethyl acetate/hexanes) to give compound **2** as a white solid (9.2 g; 71% yield), mp 98–100 °C. ^{1}H NMR ($CDCl_3$) δ 3.22 (dd, J = 15.7, 5.7 Hz, 1H), 3.34 (dd, J = 15.7, 9.4 Hz, 1H), 3.80 (s, 3H), 4.40–4.46 (m, 1H), 6.65 (s, 1H), 7.23 (d, J = 6.9 Hz, 1H), 7.38 (t, J = 7.6 Hz, 1H), 7.46 (t, J =7.6 Hz, 1H), 8.08 (d, J = 6.9 Hz, 1H); HRMS (ESI) calcd for $C_{11}H_{12}NO_3$ $[M+H]^+$ 206.0817, found 206.0811; $C_{11}H_{11}NO_3Na$ $[M+Na]^+$ 228.0637, found 228.0642.

(DL)3-(Hydroxymethyl)-3,4-dihydroisoquinolin-1(2H)-one 4—To a solution of compound **2** (4.1 g; 20.0 mmol) in dry THF (20 mL) was added dropwise a solution of 2M $LiBH_4$ in THF (10 mL; 20.0 mmol), followed by the dropwise addition of 60 mL absolute ethanol. The reaction was stirred at room temperature overnight. The reaction mixture was cooled in an ice-bath and the pH was adjusted to 4 by adding 5% HCl. The solvent was removed and the residue was treated with water (60 mL) and extracted with ethyl acetate (3 × 50 mL). The combined organic extracts were dried over anhydrous sodium sulfate. Removal of the solvent left compound **4** as a colorless oil (3.2 g, 90% yield). ^{1}H NMR ($CDCl_3$): δ 2.91 (d, J = 7.0 Hz, 2H), 3.70 (dd, J = 11.4, 4.7 Hz, 1H), 3.85 (dd, J = 11.4, 7.7 Hz, 1H), 3.85–3.96 (m, 1H), 7.20–7.48 (m, 4H), 8.02–8.05 (d, J = 7.0 Hz, 1H); HRMS (ESI) calcd for $C_{10}H_{12}NO_2$ $[M+H]^+$ 178.0868, found 178.0859; $C_{10}H_{11}NO_2Na$ $[M+Na]^+$ 200.0687, found 200.0699.

6,13-Dihydroxy-5,5a,6a,7,12,12a,13a,14-octahydrodinaphtho[2,3-a,d]-hexahydropyrazine-7,14-dione 5—A solution of 2M oxalyl chloride in CH_2Cl_2 (2.75 mL, 5.5 mmol) and 12 mL CH_2Cl_2 were placed in a 50 mL three-neck round bottom flask equipped with a thermometer, a $CaCl_2$ drying tube and two pressure-equalizing dropping funnels containing DMSO (0.85 mL; 11 mmol) in 2.5 mL CH_2Cl_2 and compound ***4*** (0.88 g; 5 mmol) in 5 mL CH_2Cl_2 and 1 mL DMSO, respectively. The DMSO solution was added to the stirred oxalyl chloride solution at −50~−60 °C. After stirring for 2 minutes, the solution containing compound ***4*** was added over 5 minutes and the mixture was stirred for an additional 15 minutes. Triethylamine (3.5 mL; 25 mmol) was added and the reaction mixture was stirred for 5 minutes and allowed to warm to room temperature for 3.5 h. Water (25 mL) was added and the two layers were separated. The aqueous layer was extracted with additional CH_2Cl_2 (25 mL) and the combined organic extracts were washed with brine (25 mL) and dried over anhydrous sodium sulfate. Removal of the solvent left a crude product which was purified by flash chromatography (silica gel/ethyl acetate/hexanes) to give compound **5** (150 mg; 8% yield) as a white solid, mp 154–156 °C. ^{1}H NMR (DMSO-D_6): δ 3.18 (dd, J = 16.6, 3.9 Hz, 2H), 3.44 (dd, J = 16.6, 6.4 Hz, 2H), 3.91 (t, J = 7.1 Hz, 2H), 4.08 (s, 2H), 5.51 (d, J = 7.6 Hz, 2H), 7.30–7.42 (m, 4H), 7.50–7.60 (t, J = 6.3 Hz, 2H), 7.79–7.83 (d, J = 6.7 Hz, 2H).

(DL)1-Oxo-1,2,3,4-tetrahydroisoquinoline-3-carboxylic acid 6—To a chilled solution of compound **2** (3.0 g; 14.7 mmol) in 30 mL THF was added 15 mL of 1 M lithium hydroxide and the reaction mixture was stirred in an ice-bath for 30 minutes. The solvent was removed on the rotary evaporator and the residue treated with water (30 mL). The solution was extracted with 50 mL ethyl acetate. The aqueous solution was acidified to pH 2, yielding a white precipitate which was collected by suction filtration and air dried to yield a white solid (2.1 g; 75% yield), mp 224–226 ° C. ^{1}H NMR (CD_3OD) δ 3.29 (dd, J = 14.3, 5.9 Hz, 1H), 3.42 (dd, J = 14.3, 5.9 Hz, 1H), 4.40 (t, J = 5.6 Hz, 1H), 7.30–7.55 (m, 3H), 7.97 (d, J = 7.8 Hz, 1H); HRMS (ESI) calcd for $C_{10}H_9NO_3Na$ $[M+Na]^+$ 214.0480, found 214.0465.

General procedure for amide 7(a–f) formation

A solution of acid **6** (0.38 g; 2 mmol) in dry N, N-dimethylformamide (5 mL) was treated with 1-[3-(dimethylamino)propyl]-3-ethylcarbodiimide hydrochloride (0.38 g; 2 mmol), followed by the appropriate amine (2 mmol). The reaction mixture was stirred at room temperature overnight. The solvent was removed in vacuo and ethyl acetate (50 mL) was added to the residue. The organic layer was washed with 5% aqueous HCl (2 × 10 mL), saturated aqueous $NaHCO_3$ (2 × 10 mL), and brine (10 mL). The organic layer was dried over anhydrous sodium sulfate, the solvent was removed on the rotary evaporator, and the

crude product was purified using flash chromatography (silica gel/ethyl acetate/hexanes) to give the corresponding amide **7a–f**.

(DL)N-(3-Methoxyphenethyl)-1-oxo-1,2,3,4-tetrahydroisoquinoline-3-carboxamide 7a—White solid (10% yield), mp 124–126 °C. ^{1}H NMR ($CDCl_3$) δ 2.60–2.72 (m, 2H), 3.20–3.30 (dd, J = 15.1, 4.4 Hz, 1H), 3.25–3.55 (m, 3H), 3.72 (s, 3H), 4.23 (q, J = 3.2 Hz, 1H), 6.52–6.72 (m, 3H), 7.02–7.50 (m, 5H), 7.60 (d, J = 2.9 Hz, 1H), 7.95 (d, J = 6.9 Hz, 1H); HRMS (ESI) calcd for $C_{19}H_{21}N_2O_3$ $[M+H]^+$ 325.1552, found 325.1547; $C_{19}H_{20}N_2O_3Na$ $[M+Na]^+$ 347.1372, found 347.1364.

(DL)N-(2-Morpholinoethyl)-1-oxo-1,2,3,4-tetrahydroisoquinoline-3-carboxamide 7b—White solid (26% yield), mp 138–140 °C. ^{1}H NMR (CD_3OD) δ 2.28–2.52 (m, 6H), 3.20–3.38 (m, 2H), 3.60 (t, J = 5.0 Hz, 4H), 3.72(s, 2H), 4.26 (t, J = 5.6 Hz, 1H), 7.27 (d, J = 6.9 Hz, 1H), 7.35 (t, J = 7.5 Hz, 1H), 7.46 (t, J = 7.6 Hz, 1H), 7.92 (d, J = 6.9 Hz, 1H); HRMS (ESI) calcd for $C_{16}H_{22}N_3O_3$ $[M+H]^+$ 304.1661, found 304.1652.

(DL)N-(Furan-2-ylmethyl)-1-oxo-1,2,3,4-tetrahydroisoquinoline-3-carboxamide 7c—White solid (57% yield), mp 157–158 °C. ^{1}H NMR ($CDCl_3$) δ 3.30 (dd, J = 15.6, 5.2 Hz, 1H), 3.43 (dd, J = 15.6, 5.2 Hz, 1H), 4.26–4.33 (m, 1H), 4.32 (dd, J = 14.3, 5.8 Hz, 1H), 4.46 (dd, J = 14.3, 5.8 Hz, 1H), 6.01 (d, J = 1.9 Hz, 1H), 6.22–6.24 (m, 1H), 6.55 (s, 2H), 7.20–7.55 (m, 4H), 7.99–8.02 (d, J = 5.9 Hz, 1H); HRMS (ESI) calcd for $C_{15}H_{15}N_2O_3$ $[M+H]^+$ 271.1083, found 271.1068; $C_{15}H_{14}N_2O_3Na$ $[M+Na]^+$ 293.0902, found 293.0894.

(DL)N-(2,2-Diphenylethyl)-1-oxo-1,2,3,4-tetrahydroisoquinoline-3-carboxamide 7d—White solid (23% yield), mp 166–168 °C. ^{1}H NMR ($CDCl_3$) δ 3.16 (dd, J = 16.9, 5.8 Hz, 1H), 3.34 (dd, J = 16.9, 6.8 Hz, 1H), 3.65–3.80 (m, 1H), 3.85–4.00 (m, 1H), 4.00–4.12(m, 1H), 4.12–4.20 (m, 1H), 4.58 (s, 1H), 4.68 (s, 1H), 6.98–7.52 (m, 13H), 7.85–7.92 (d, J = 9.4 Hz, 1H); HRMS (ESI) calcd for $C_{24}H_{23}N_2O_2$ $[M+H]^+$ 371.1760, found 371.1761; $C_{24}H_{22}N_2O_2Na$ $[M+Na]^+$ 393.1579, found 393.1580.

(DL)N-Hexyl-1-oxo-1,2,3,4-tetrahydroisoquinoline-3-carboxamide 7e—White solid (24% yield), mp 99–101°C. ^{1}H NMR ($CDCl_3$) δ 0.79 (t, J = 7.3 Hz, 3H), 1.09–1.20 (m, 2H), 1.30–1.41(m, 2H), 3.18–3.23 (m, 2H), 3.31 (dd, J = 13.9, 5.0 Hz, 1H), 3.45 (dd, J = 13.9, 5.0 Hz, 1H), 4.26 (q, J = 3.8 Hz, 1H), 6.62 (s, 1H), 7.24 (d, J = 8.4 Hz, 1H), 7.36 (t, J = 7.8 Hz, 1H), 7.46 (t, J = 7.8 Hz, 1H), 7.52 (s, 1H), 7.98 (d, J = 8.3 Hz, 1H); HRMS (ESI) calcd for $C_{14}H_{18}N_2O_2Na$ $[M+Na]^+$ 269.1266, found 269.1276; $C_{14}H_{18}N_2O_2K$ $[M+K]^+$ 285.1005, found 285.1012.

(DL) N-Benzyl-1-oxo-1,2,3,4-tetrahydroisoquinoline-3-carboxamide 7f—White solid (110 mg; 20% yield), mp 165–167 °C. $_1$H NMR ($CDCl_3$) δ 3.30 (dd, J = 15.8, 6.2 Hz, 1H), 4.46 (dd, J = 15.8, 6.2 Hz, 1H), 4.26 (t, J = 3.4 Hz, 1H), 4.31 (dd, J = 13.5, 5.1 Hz, 1H), 4.44 (dd, J = 13.5, 5.1 Hz, 1H), 6.82 (s, 1H), 6.89–7.54 (m, 9H), 7.91 (d, J = 7.4 Hz, 1H); HRMS (ESI) calcd for $C_{17}H_{17}N_2O_2$ $[M+H]^+$ 281.1290, found 281.1275; $C_{17}H_{16}N_2O_2Na$ $[M+Na]^+$ 303.1109, found 303.1097.

General procedure for N-Boc/N-Cbz phenylalanine and aromatic amine coupling reactions

DL-N-Cbz-phenylalanine (or L-N-Boc-phenylalanine) (5 mmol) was dissolved in 10 mL DMF and 1-[3-(dimethylamino)propyl]-3-ethylcarbodiimide hydrochloride (0.96 g; 5 mmol) was added, followed by the appropriate aromatic amine (5.5 mmol). The resulting mixture was stirred at room temperature overnight. Removal of the solvent on the rotary evaporator left a residue which was dissolved in 50 mL ethyl acetate. The ethyl acetate solution was washed with 5% aqueous HCl (3 × 25 mL), saturated aqueous $NaHCO_3$ (3 × 25 mL), and

brine (25 mL). The organic layer was dried over anhydrous sodium sulfate and the solvent was removed on the rotary evaporator to give pure product **8**.

(DL)Tert-butyl 1-oxo-3-phenyl-1-(thiazol-2-ylamino)propan-2-yl-carbamate 8g—White solid (63% yield), mp 88–90 °C. ^{1}H NMR ($CDCl_3$) δ 1.40 (s, 9H), 3.05–3.20 (m, 2H), 4.64–4.78 (m, 1H), 5.18 (s, 1H), 7.00–7.28 (m, 6H), 7.54 (d, J = 2.2 Hz, 1H), 11.20 (s, 1H); HRMS (ESI) calcd for $C_{17}H_{22}N_3O_3S$ $[M+H]^+$ 348.1382, found 348.1368; $C_{17}H_{21}N_3O_3Na$ $[M+Na]^+$ 370.1201, found 370.1190.

(DL)Benzyl 1-(benzo[d][1,3]dioxol-5-ylamino)-1-oxo-3-phenylpropan-2-yl-carbamate 8h—White solid (48% yield), mp 145–147 °C. ^{1}H NMR ($CDCl_3$) δ 3.02–3.20 (m, 2H), 4.50 (q, J = 7.8 Hz, 1H), 5.05 (s, 2H), 5.50 (s, 1H), 5.92 (s, 2H), 6.61 (dd, J = 36.5, 7.2 Hz, 2H), 7.03 (s, 1H), 7.18–7.37 (m, 10H), 7.55 (s, 1H); HRMS (ESI) calcd for $C_{24}H_{23}N_2O_5$ $[M+H]^+$ 419.1607, found 419.1594; $C_{24}H_{22}N_2O_5Na$ $[M+Na]^+$ 441.1426, found 441.1412.

(DL)Benzyl 1-(4-morpholinophenylamino)-1-oxo-3-phenylpropan-2-yl-carbamate 8i—White solid (87% yield), mp 200–202 °C. ^{1}H NMR ($CDCl_3$) δ 3.05–3.22 (m, 6H), 3.85 (t, J = 4.3 Hz, 4H), 4.51 (q, J = 5.9 Hz, 1H), 5.08 (s, 2H), 5.48 (s, 1H), 6.80 (dd, J = 9.4 Hz, 2H), 7.18–7.38 (m, 12H), 7.40 (s, 1H); HRMS (ESI) calcd for $C_{27}H_{30}N_3O_4$ $[M+H]^+$ 460.2236, found 460.2198; $C_{27}H_{29}N_3O_4Na$ $[M+Na]^+$ 482.2056, found 482.2047.

(DL)Benzyl 1-oxo-1-(3-phenoxyphenylamino)-3-phenylpropan-2-ylcarbamate 8j—White solid (100% yield), mp 132–134 °C. ^{1}H NMR ($CDCl_3$) δ 3.02–3.20 (m, 2H), 4.45–4.58 (m, 1H), 5.05 (s, 2H), 5.48 (s, 1H), 6.37–6.42 (m, 1H), 6.70–6.75 (m, 1H), 6.98–7.37 (m, 19H), 7.68 (s, 1H); HRMS (ESI) calcd for $C_{29}H_{27}N_2O_4$ $[M+H]^+$ 467.1971, found 467.1963; $C_{29}H_{26}N_2O_4Na$ $[M+Na]^+$ 489.1790, found 489.1777.

(DL)1-Oxo-N-(thiazol-2-yl)-1,2,3,4-tetrahydroisoquinoline-3-carboxamide 7g—Compound ***8g*** (1.14 g; 3.28 mmol) was dissolved in 15 mL trifluoroacetic acid at room temperature. The reaction mixture was stirred for 30 minutes and the trifluoroacetic acid was removed under vacuum. Water (5 mL) was added and the pH was adjusted to 9 using a saturated solution of sodium carbonate. The free amine was extracted with 50 mL ethyl acetate and the organic layer was dried using anhydrous sodium sulfate. Removal of the solvent left a colorless oil (0.60 g; 74% yield). The oil was dissolved in 10 mL dioxane, and trichloromethyl chloroformate (0.4 mL; 3.4 mmol) was added. The resulting mixture was stirred at room temperature overnight. Removal of the solvent under vacuum left a residue which was dissolved in methylene chloride (20 mL). Aluminum chloride (0.64 g; 4.8 mmol) was added and the resulting mixture was refluxed for 1h. The reaction mixture was allowed to cool to room temperature and water (10 mL) was slowly added. The mixture was stirred for 30 minutes and then transferred to a separatory funnel. The organic layer was washed with water (2 × 15 mL) and dried over anhydrous sodium sulfate. Removal of the solvent gave a pure product ***7g*** (50 mg; 6% yield) as a gray solid, mp 202–204 °C. ^{1}H NMR ($CDCl_3$) δ 2.96 (dd, J = 13.2, 9.0 Hz, 1H), 3.45 (dd, J = 12.0, 2.4 Hz, 1H), 4.40–4.48 (m, 1H), 5.58 (s, 1H), 7.20–7.38 (m, 6H), 7.77 (d, J = 1.3 Hz, 1H); HRMS (ESI) calcd for $C_{13}H_{12}N_3O_2S$ $[M+H]^+$ 274.0650, found 274.0659; $C_{13}H_{11}N_3O_2SNa$ $[M+Na]^+$ 296.0470, found 296.0468.

Representative procedure for the synthesis of compounds 7h-j

(DL)N-(Benzo[d][1,3]dioxol-5-yl)-1-oxo-1,2,3,4-tetrahydroisoquinoline-3-carboxamide 7h—Compound ***8h*** (1.0 g; 2.39 mmol) was dissolved in 50 mL ethyl acetate, then 10% palladium/carbon(0.33 g) wetted with 2 mL ethyl acetate was added. The

mixture was placed on a Parr hydrogenator, 20 psi hydrogen gas was applied and the mixture was shaken for 3 h. The reaction mixture was gravity filtered and the filtrate was evaporated to give a brown oil (0.5g; 74% yield) which was dissolved in 8 mL 1, 4-dioxane and treated with trichloromethyl chloroformate (0.3 mL; 2.5 mmol). The resulting mixture was stirred at room temperature overnight. The solvent was removed under vacuum and the residue was taken up in methylene chloride (15 mL). Aluminum chloride (0.48 g; 3.6 mmol) was added and the resulting mixture was refluxed for 1 h and allowed to cool to room temperature. After water (15 mL) was slowly added, the reaction mixture was stirred for 30 minutes and then transferred to a separatory funnel. The organic layer was washed with water (2 × 15 mL) and dried over anhydrous sodium sulfate. Removal of the solvent left a crude product which was purified by flash chromatography (silica gel/ethyl acetate/hexanes) to give compound ***7h*** (120 mg; 16% yield) as a white solid, mp 120–122 °C. ^{1}H NMR ($CDCl_3$) δ 3.09 (dd, J = 13.2, 3.6 Hz, 1H), 3.20 (dd, J = 13.2, 5.7 Hz, 1H), 4.35–4.40 (m, 1H), 5.95 (s, 2H), 6.50–6.59 (m, 2H), 6.81 (d, J = 7.6 Hz, 1H), 6.88 (s, 1H), 7.20–7.35 (m, 5H); HRMS (ESI) calcd for $C_{17}H_{15}N_2O_4$ $[M+H]^+$ 311.1032, found 311.1037; $C_{17}H_{14}N_2O_4Na$ $[M+Na]^+$ 333.0851, found 333.0840.

(DL)N-(4-(1,3-Oxazinan-3-yl)phenyl)-1-oxo-1,2,3,4-tetrahydroisoquinoline-3-carboxamide 7i—White solid (5% yield), mp 166–168 °C. ^{1}H NMR ($CDCl_3$) δ 3.01–3.35 (m, 6H), 3.85 (t, J = 5.0 Hz, 4H), 4.37–4.41(m, 1H), 6.04 (s, 1H), 6.92 (d, J = 9.4 Hz, 2H), 7.05 (d, J = 9.4 Hz, 2H), 7.22–7.38 (m, 4H); HRMS (ESI) calcd for $C_{20}H_{22}N_3O_3$ $[M+H]^+$ 352.1661, found 352.1648; $C_{20}H_{21}N_3O_3Na$ $[M+Na]^+$ 374.1481, found 374.1467.

(DL)1-Oxo-N-(3-phenoxyphenyl)-1,2,3,4-tetrahydroisoquinoline-3-carboxamide 7j—White solid (7% yield), mp 93–95 °C. ^{1}H NMR ($CDCl_3$) δ 3.06 (dd, J = 10.3, 5.1 Hz, 1H), 3.27 (dd, J = 10.3, 2.5 H, 1H), 4.38–4.40 (m, 1H), 6.22 (s, 1H), 6.82–7.40 (m, 14H); HRMS (ESI) calcd for $C_{22}H_{19}N_2O_3$ $[M+H]^+$ 359.1396, found 359.1398; $C_{22}H_{18}N_2O_3Na$ $[M+Na]^+$ 381.1215, found 381.1219.

Methyl 1-oxo-1,2-dihydroisoquinoline-3-carboxylate 9—To a solution of compound 1-oxo-1, 2, 3, 4-tetrahydroisoquinoline 3-carboxymethyl ester ***2*** (13.61 g; 66 mmol) in 200 mL 1, 4-dioxane was added 2,3-dichloro-5,6-dicyanobenzoquinone (DDQ) (16.0g; 70.5 mmol) and the mixture was refluxed overnight. The solvent was removed *in vacuo* and the residue was taken up in 200 mL ethyl acetate and washed with 5% NaOH (2 × 50 mL). The organic layer was dried over anhydrous sodium sulfate and the filtrate was evaporated, leaving a crude product which was purified with flash chromatography (silica gel/ethyl acetate/hexanes) to give compound ***9*** as a white solid (3.0 g; 22% yield), mp 154–155 °C. ^{1}H NMR ($CDCl_3$) δ 3.92 (s, 3H), 7.52–7.68 (m, 4H), 8.37–8.41 (m, 1H), 9.12 (s, 1H); HRMS (ESI) calcd for $C_{11}H_{10}NO_3$ $[M+H]^+$ 204.0661, found 204.0664; $C_{11}H_9NO_3Na$ $[M+Na]^+$ 226.0480, found 226.0475.

Methyl 4-bromo-1-oxo-1,2-dihydroisoquinoline-3-carboxylate 11—To a solution of compound 1-oxo-1, 2, 3, 4-tetrahydroisoquinoline 3-carboxymethyl ester ***2*** (3.56 g; 17.4 mmol) in 175 mL methylene chloride were added N-bromosuccinimide (NBS) (6.26 g; 35.2 mmol) and benzyl peroxide (0.20 g; 0.8 mmol), and the reaction was refluxed for 24 h. The reaction was cooled down to room temperature and then washed with saturated $NaHCO_3$ (3 × 80 mL) and brine (80 mL). The organic layer was dried over anhydrous sodium sulfate. The drying agent was filtered and the filtrate was concentrated. The crude product was precipitated in 30 mL ethyl acetate and filtered, yielding compound ***11*** as a white solid (2.84 g; 57% yield), mp 186–187 °C. ^{1}H NMR ($CDCl_3$) δ 4.05 (s, 3H), 7.68 (t, J = 8.1 Hz, 1H), 7.85 (t, J = 8.1 Hz, 1H), 8.27 (d, J = 6.5 Hz, 1H), 8.46 (d, J = 6.5 Hz, 1H), 9.45 (s, 1H); HRMS (ESI) calcd for $C_{11}H_9$ $^{35}BrNO_3$ $[M+H]^+$ 281.9766, found 281.9767; $C_{11}H_9$ $^{37}BrNO_3$

$[M+H]^+$ 283.9745, found 283.9744; $C_{11}H_8\ ^{35}BrNO_3Na$ $[M+Na]^+$ 303.9585, found 303.9584; $C_{11}H_8\ ^{37}BrNO_3Na$ $[M+Na]^+$ 305.9565, found 305.9569.

Hydrolysis of methyl ester 9—To a solution of ester ***9*** (5 mmol) in 10 mL dioxane was added 1M lithium hydroxide (10 mL), and the reaction mixture was stirred at room temperature for 1 h. The solvent was removed on the rotary evaporator and the residue was treated with 20 mL water and acidified to pH 2, forming a precipitate. The precipitate was collected by suction filtration and washed with 20 mL ethyl acetate to give the corresponding acid as a white solid (80% yield), mp 230–232 °C. ^{1}H NMR (DMSO-D_6) δ 7.40 (s, 1H), 7.64 (t, J = 7.3 Hz, 1H), 7.79 (t, J = 7.3 Hz, 1H), 7.85 (d, J = 7.5 Hz, 1H), 8.22 (d, J = 7.5 Hz, 1 H), 11.80 (s, 1H).

The acid derived from ester ***11*** was obtained the same procedure as that above. White solid (64% yield), mp > 260 °C. ^{1}H NMR (DMSO-D_6) δ 7.69 (t, J = 6.9 Hz, 1H), 7.84–8.00 (m, 2H), 8.25 (d, J = 5.3 Hz, 1H), 11.80 (s, 1H).

General coupling reaction procedure for compounds 10c, 10f, 12a, 12c, 12f and 12i-j

A solution of acid (2 mmol) derived from ***9*** or ***11*** in dry N, N-dimethylformamide (5 mL) was treated with 1-[3-(dimethylamino)propyl]-3-ethylcarbodiimide hydrochloride (EDCI) (0.38 g; 2 mmol), followed by the appropriate amine (2 mmol). The reaction mixture was stirred at room temperature overnight. The solvent was removed under vacuum and the residue was added ethyl acetate (30 mL). The organic layer was washed with 5% aqueous HCl (3 × 10 mL), saturated aqueous $NaHCO_3$ (3 ×10 mL), and brine (10 mL). The organic layer was dried over anhydrous sodium sulfate. The drying agent was filtered and the solvent was removed. The crude product was purified by flash chromatography (silica gel/ethyl acetate/hexanes) to give compounds ***10c, 10f, 12a, 12c, 12f and 12i-j***.

N-(Furan-2-ylmethyl)-1-oxo-1,2-dihydroisoquinoline-3-carboxamide 10c—White solid (10% yield), mp 138–140 °C. ^{1}H NMR (DMSO-D_6) δ 4.48 (s, 2H), 6.34–6.36 (m, 1H), 6.60–6.62 (m, 1H), 7.35 (s, 1H), 7.57–7.80 (m, 4H), 8.22 (d, J = 8.3 Hz, 1H); HRMS (ESI) calcd for $C_{15}H_{13}N_2O_3$ $[M+H]^+$ 269.0926, found 269.0936; $C_{15}H_{12}N_2O_3Na$ $[M+Na]^+$ 291.0746, found 291.0752.

N-Benzyl-1-oxo-1,2-dihydroisoquinoline-3-carboxamide 10f—White solid(15% yield), mp 189–191 °C. ^{1}H NMR ($CDCl_3$) δ 4.70 (d, J = 3.5 Hz, 2H), 7.20–7.72 (m, 9H), 8.08 (d, J = 7.7 Hz, 1H), 10.88 (s, 1H); HRMS (ESI) calcd for $C_{17}H_{15}N_2O_2$ $[M+H]^+$ 279.1134, found 279.1130; $C_{17}H_{14}N_2O_2Na$ $[M+Na]^+$ 301.0953, found 301.0960.

4-Bromo-N-(3-methoxyphenethyl)-1-oxo-1,2-dihydroisoquinoline-3-carboxamide 12a—White solid (18% yield), mp 175–177 °C. ^{1}H NMR ($CDCl_3$) δ 2.97 (t, J = 6.9 Hz, 2H), 3.82 (s, 3H), 3.80–3.86 (m, 2H), 6.80–6.89 (m, 3H), 7.23–7.30 (m, 1H), 7.64 (t, J = 7.1 Hz, 1H), 7.67 (s, 1H), 7.79 (t, J = 7.1 Hz, 1H), 8.03 (d, J = 7.4 Hz, 1H), 8.45 (d, J = 7.4 Hz, 1H), 9.78 (s, 1H); HRMS (ESI) calcd for $C_{19}H_{18}\ ^{35}BrN_2O_3$ $[M+H]^+$ 401.0501, found 401.0502; $C_{19}H_{18}\ ^{37}BrN_2O_3$ $[M+H]^+$ 403.0480, found 403.0480; $C_{19}H_{17}\ ^{35}BrN_2O_3Na$ $[M+Na]^+$ 423.0320, found 423.0320; $C_{19}H_{17}\ ^{37}BrN_2O_3Na$ $[M+Na]^+$ 425.0300, found 425.0297.

4-Bromo-N-(furan-2-ylmethyl)-1-oxo-1,2-dihydroisoquinoline-3-carboxamide 12c—White solid (15% yield), mp 197–199 °C. ^{1}H NMR ($CDCl_3$) δ 4.70 (d, J = 4.7 Hz, 2H), 6.37 (s, 2H), 7.41 (m, 1H), 7.64 (t, J = 9.4 Hz, 1H), 7.80 (t, J = 9.4 Hz, 1H), 8.00 (s, 1H), 8.05 (d, J = 9.9 Hz, 1H), 8.42 (d, J = 9.9 Hz, 1H), 9.90 (s, 1H); HRMS (ESI) calcd for $C_{15}H_{12}\ ^{35}BrN_2O_3$ $[M+H]^+$ 347.0031, found 347.0029; $C_{15}H_{12}\ ^{37}BrN_2O_3$ $[M+H]^+$

349.0011, found 348.9997; $C_{15}H_{11}$ $^{35}BrN_2O_3Na$ $[M+Na]^+$ 368.9851, found 368.9850; $C_{15}H_{11}$ $^{37}BrN_2O_3Na$ $[M+Na]^+$ 370.9830, found 370.9820.

N-Benzyl-4-bromo-1-oxo-1,2-dihydroisoquinoline-3-carboxamide 12f—White solid (45% yield), mp 208–209 °C. ^1H NMR (DMSO-D_6) δ 4.48 (d, J = 3.7 Hz, 2H), 7.23–8.27 (m, 9H), 9.33 (t, J = 3.3 Hz, 1H), 12.10 (s, 1H); HRMS (ESI) calcd for $C_{17}H_{14}$ $^{35}BrN_2O_2$ $[M+H]^+$ 357.0239, found 357.0236; $C_{17}H_{14}$ $^{37}BrN_2O_2$ $[M+H]^+$ 359.0218, found 359.0235; $C_{17}H_{13}$ $^{35}BrN_2O_2Na$ $[M+Na]^+$ 379.0058, found 379.0059; $C_{17}H_{13}$ $^{37}BrN_2O_2Na$ $[M+Na]^+$ 381.0038, found 381.0041.

4-Bromo-N-(4-morpholinophenyl)-1-oxo-1,2-dihydroisoquinoline-3-carboxamide 12i—White solid (10% yield), mp 252–254 °C. ^1H NMR (DMSO-D_6) δ 3.05–3.15 (m, 4H), 3.70–3.80 (m, 4H), 6.96 (d, J = 7.3 Hz, 2H), 7.56 (d, J = 7.3 Hz, 2H), 7.60–7.68 (m, 1H), 7.84–7.96 (m, 2H), 8.26 (d, J = 6.9 Hz, 1H), 10.82 (s, 1H), 12.17 (s, 1H); HRMS (ESI) calcd for $C_{20}H_{19}$ $^{35}BrN_3O_3$ $[M+H]^+$ 428.0610, found 428.0625; $C_{20}H_{19}$ $^{37}BrN_3O_3$ $[M+H]^+$ 430.0589, found 430.0592; $C_{20}H_{18}$ $^{35}BrN_3O_3Na$ $[M+Na]^+$ 450.0429, found 450.0453; $C_{20}H_{18}$ $^{37}BrN_3O_3Na$ $[M+Na]^+$ 452.0409, found 452.0429.

4-Bromo-1-oxo-N-(3-phenoxyphenyl)-1,2-dihydroisoquinoline-3- carboxamide 12j—White solid (33% yield), mp 216–218 °C. ^1H NMR (DMSO-D_6) δ 6.78 (d, J = 7.4 Hz, 1H), 7.04 (d, J = 7.4 Hz, 2H), 7.13 (d, J = 7.0 Hz, 1H), 7.27–7.40 (m, 3H), 7.46–7.64 (m, 3H), 7.82 (t, J = 7.4 Hz, 1H), 8.00 (d, J = 7.5 Hz, 1H), 8.40 (d, J = 7.5 Hz, 1H), 10.50 (s, 1H), 11.72 (s, 1H); HRMS (ESI) calcd for $C_{22}H_{16}$ $^{35}BrN_2O_3$ $[M+H]^+$ 435.0344, found 435.0340; $C_{22}H_{16}$ $^{37}BrN_2O_3$ $[M+H]^+$ 437.0324, found 437.0341; $C_{22}H_{15}$ $^{35}BrN_2O_3Na$ $[M+Na]^+$ 457.0164, found 457.0155; $C_{22}H_{15}$ $^{37}BrN_2O_3Na$ $[M+Na]^+$ 459.0143, found 459.0146.

WNV NS2B/NS3 protease assays (14)—All assays were performed in opaque 96-well plates. Reaction mixtures (100 μL/assay) contained 200 mM TRIS buffer, pH 9.5, 13.5 mM NaCl, 30% glycerol, 0.025 μM enzyme, and 100 μM fluorogenic peptide substrate (Boc-Gly-Lys-Arg-7-amino-4-methyl coumarin). Enzyme incubations were at 25 °C for 30 minutes. The fluorescence of 7-amino-4-methyl coumarin (AMC) released from the cleavage of the substrate was monitored using excitation and emission wavelengths of 385 nm and 465 nm, respectively.

WNV NS2B/NS3 protease inhibition assays (14)—The protease inhibitor assays contained 200 mM Tris-HCl buffer, pH 9.5, 13.5 mM NaCl, 30% glycerol, 0.025 μM enzyme (2.5 pmol), 100 μM fluorogenic peptide substrate and 50 μM inhibitor. The inhibitors were dissolved in DMSO and diluted in assay buffer. The DMSO concentration in the assay mix was maintained at 1%, including in the no-inhibitor control. The assay mixtures containing WNV protease with an inhibitor (or without the inhibitor as a control) were pre-incubated at room temperature for fifteen minutes. An aliquot of the substrate (100 μM) was added and the incubation continued for an additional fifteen minutes. Fluorescence values were obtained using excitation and emission wavelengths of 385 nm and 465 nm, respectively. The percent inhibition of protease activity was determined using Microsoft Excel. For calculation of IC50 value, in vitro protease assays were performed in triplicate as described above in the presence of 10, 20, 30, 40 and 50 μM of compound ***12j*** or no-compound control. The % inhibition (y-axis) was plotted against the concentration of the inhibitor (x-axis) using GraphPad Prism 5.0 software.

Molecular modeling—Molecular docking simulations were performed via the AutoDock program (31). Compound ***12j*** was constructed in SYBYL 8.0 (32) and structurally optimized

to default convergence thresholds using the Tripos Force Field (33) and Gasteiger-Marsili partial atomic charges (34). The active site model for WNV protease was prepared using the 2FP7 crystal structure (16). The structure was protonated in SYBYL, stripped of all water molecules and bound ligands, and electrostatically represented with Gasteiger-Marsili charges. AutoDock simulations were performed using the Lamarckian Genetic Algorithms (GA) subroutine at default settings for GA population size, cross-over rate and mutation rate, and starting with fully-randomized ligand position, orientation and conformation. One hundred GA runs were performed for the ligand-enzyme pair.

Acknowledgments

This work was supported by the National Institutes of Health (AI577045 and AI 070791).

References and Notes

1. Abbenante G, Fairlie DP. Med Chem. 2005; 1:71–104. [PubMed: 16789888]
2. Maly DJ, Huang L, Ellman JA. Chem Biochem. 2002; 3:16–37.
3. Burke, SD.; Monath, TP. Flaviviruses in Field's. In: Knipe, DM., et al., editors. Virology. 4. Lippincott, Williams & Wilkins; Philadelphia, PA: 2001.
4. (a) Ray D, Shi PY. Recent Pat Anti-infect Drug Discov. 2006; 1:45–55. (b) Chapell KJ, Stoermer MJ, Fairlie DP, Young PR. J Biol Chem. 2006; 281:38448–38458. [PubMed: 17052977]
5. (a) Chappell KJ, Stoermer MJ, Fairlie DP, Young PR. Curr Med Chem. 2008; 15:2771–2784. [PubMed: 18991636] (b) Sampath A, Padmanabhan R. Antiviral Res. 2009; 81:6–15. [PubMed: 18796313] (c) Steuber H, Hilgenfeld R. Curr Top Med Chem. 2010; 10:323–345. [PubMed: 20166951] (d) Diamond MS. Antiviral Res. 2009; 83:214–227. [PubMed: 19501622]
6. Clum S, Ebner KE, Padmanabhan R. J Biol Chem. 1997; 272:30715–30723. [PubMed: 9388208]
7. Lindenbach BD, Rice CM. Adv Virus Res. 2003; 59:23–61. [PubMed: 14696326]
8. Padmanabhan R, Mueller N, Reichert E, Yon C, Teramoto T, Kono Y, Takhampunya R, Ubol S, Pattabiraman N, Falgout B, Ganesh VK, Murthy K. Novartis Found Symp. 2006; 277:74–84. [PubMed: 17319155]
9. Nomenclature used is that of Schechter I, Berger A. Biochem Biophys Res Comm. 1967; 27:157–162. [PubMed: 6035483] , where S_1, S_2, S_3,… S_n and S_1', S_2', S_3',… S_n' correspond to the enzyme subsites on either side of the scissile bond. Each subsite accommodates a corresponding amino acid residue side chain designated P_1, P_2, P_3, …. P_n and P_1', P_2', P_3', …. P_n' of the substrate or (inhibitor). S1 is the primary substrate specificity subsite, and P_1-P_1' is the scissile bond.
10. Falgout B, Miller RH, Lai CJ. J Virol. 1993; 67:2034–2042. [PubMed: 8383225]
11. Chambers TJ, Nestorowicz A, Amberg SM, Rice CM. J Virol. 1993; 67:6797–807. [PubMed: 8411382]
12. Yusof RS, Clum M, Wetzel H, Murthy M, Padmanabhan R. J Biol Chem. 2000; 265:9963–9. [PubMed: 10744671]
13. Chambers TJ, Hahn CS, Galler R, Rice CM. Ann Rev Microbiol. 1990; 44:649–688. [PubMed: 2174669]
14. Mueller NH, Yon C, Ganesh VK, Padmanabhan R. Int J Biochem Cell Biol. 2007; 39:606–614. [PubMed: 17188926]
15. Aleshin AE, Shiryaev SA, Strongin AY, Liddington RC. Protein Sci. 2007; 16:795–806. [PubMed: 17400917]
16. Erbel P, Schiering N, D'Arcy A, Renatus M, Kroemer M, Lim SP, Yin Z, Keller TH, Vasudevan SG, Hommel U. Nature Str Mol Biol. 2006; 13:372–373.
17. (a) Knox JE, Ma NL, Yin Z, Patel SJ, Wang WL, Chan WL, Rao KRR, Ngew X, Patel V, Beer D, Lim SP, Vasudevan SG, Keller TH. J Med Chem. 2006; 49:6585–6590. [PubMed: 17064076] (b) Stoermer MJ, Chappell KJ, Liebscher S, Jensen CM, Gan CH, Gupta PK, Xu WJ, Young PR, Fairlie DP. J Med Chem. 2008; 51:5714–5721. [PubMed: 18729351]

18. Shiryaev SA, Ratnikov BI, Chakanov AV, Sikora S, Rozanov DV, Godzik A, Wang J, Smith JW, Huang Z, Lindberg I, Samuel MS, Diamond MS, Strongin AY. Biochem J. 2006; 393:503–511. [PubMed: 16229682]
19. Ganesh VK, Mueller N, Judge K, Luan CH, Padmanabhan R, Murthy KHM. Bioorg Med Chem. 2005; 13:257–264. [PubMed: 15582469]
20. Goodell JR, Puig-Basagoiti, Forshey BM, Shi P-Y, Ferguson DM. J Med Chem. 2006; 49:2127–2137. [PubMed: 16539402]
21. Barklis E, Still A, Sabri MI, Hirsch AJ, Nikolich-Zugich J, Brien J, Dhenub TC, Scholz I, Alfadhli A. Antimicrobial Agents Chemoth. 2007; 51:2642–2645.
22. (a) Noueiry AO, Olivo PD, Slomenzyska U, Zhou Y, Buscher B, Geiss B, Engle M, Roth RM, Chung KM, Samuel M, Diamond MS. J Virol. 2007; 81:11992–12004. [PubMed: 17715228] (b) Ekonomiuk D, Su XC, Ozawa K, Bodenreider C, Lim SP, Yin Z, Keller TH, Beer D, Patel V, Otting G, Caflisch A, Huang D. PLoS Negl Trop Dis. 2009; 3(1):e-356. [PubMed: 19159012]
23. Hein GE, Niemann K. J Am Chem Soc. 1962; 84:4487–4494.
24. Zhong J, Groutas WC. Curr Top Med Chem. 2004; 4:1203–1216. [PubMed: 15320721]
25. Zakharkin LI, Khorlina IM. Tetrahedron Lett. 1962:619–620.
26. Chandrasekhar S, Kumar MS, Muralidhar B. Tetrahedron Lett. 1998:909–910.
27. Cha JS, Kwon SS. J Org Chem. 1987; 52:5487–5489.
28. Mancuso AJ, Huang SL, Swern D. J Org Chem. 1978; 43:2480–2482.
29. Boger DL, Miyauchi H, Du W, Hardouin C, Fecik RA, Cheng H, Hwang I, Hedrick MP, Leung D, Acevedo O, Guimaraes CRW, Jorgensen WL, Cravatt BF. J Med Chem. 2005; 48:1849–1856. [PubMed: 15771430]
30. (a) Huang W, Yamamoto Y, Li Y, Dou D, Alliston KR, Hanzlik RP, Williams TD, Groutas WC. J Med Chem. 2008; 51:2003–2008. and references cited therein. [PubMed: 18318470] (b) Li Y, Yang Q, Dou D, Alliston KR, Groutas WC. Bioorg Med Chem. 2008; 16:692–698. [PubMed: 17976994] (c) Lai Z, Gan X, Wei L, Alliston KR, Yu H, Li YH, Groutas WC. Arch Biochem Biophys. 2004; 429:191–197. [PubMed: 15313222] (d) Zhong J, Gan X, Alliston KR, Lai Z, Yu H, Groutas CS, Wong T, Groutas WC. J Comb Chem. 2004; 6:556–563. [PubMed: 15244417] (e) Kuang R, Epp JB, Ruan S, Yu H, Huang P, He S, Tu J, Schechter NM, Turbov J, Froleich CJ, Groutas WC. J Am Chem Soc. 1999; 121:8128–8129.
31. Morris GM, Goodsell DS, Halliday RS, Huey R, Hart WE, Belew RK, Olson AJ. J Comput Chem. 1998; 19:1639–1662.
32. SYBYL 8.0. The Tripos Associates; St. Louis MO: 2008.
33. Clark M, Cramer RD III, Van Opdenbosch N. J Comput Chem. 1989; 10:982–1012.
34. Gasteiger J, Marsili M. Tetrahedron Lett. 1978:3181–3184.

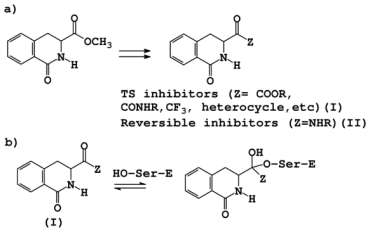

Figure 1.

(a) Design of transition state inhibitors (I) based on the 1-oxo-1, 2, 3, 4-tetrahydroisoquinoline scaffold; (b) Postulated mechanism of action of (I).

Figure 2(a)

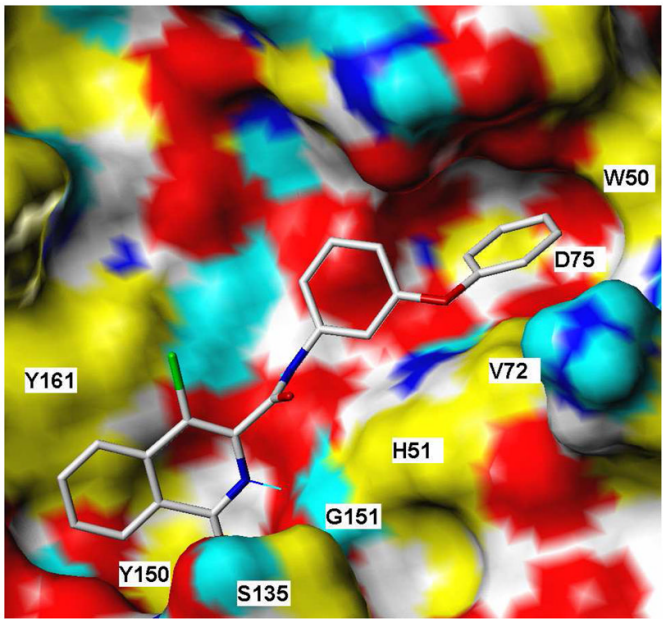

Figure 2(b)

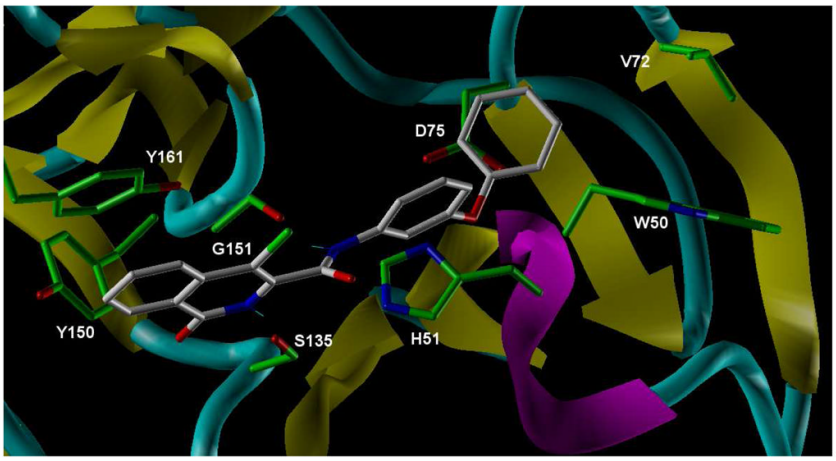

Figure 2.

(a) Predicted binding of energy-minimized compound ***12j*** docked to the binding site of WNV protease. The enzyme surface is colored as follows: red polar O, blue = polar N, cyan = donatable H, white = mildly polar H/C, yellow = nonpolar H/C/S. (b) Conformer of compound ***12j*** in the proteolytic active site of WNV protease as predicted by molecular docking simulations. The ligand is shown as CPK-colored sticks with white carbon atoms, while a number of key interacting receptor residues are rendered similarly but with green carbons. The overall structure of the protein is depicted via secondary structure elements (purple helices, yellow sheets/strands, and cyan coils).

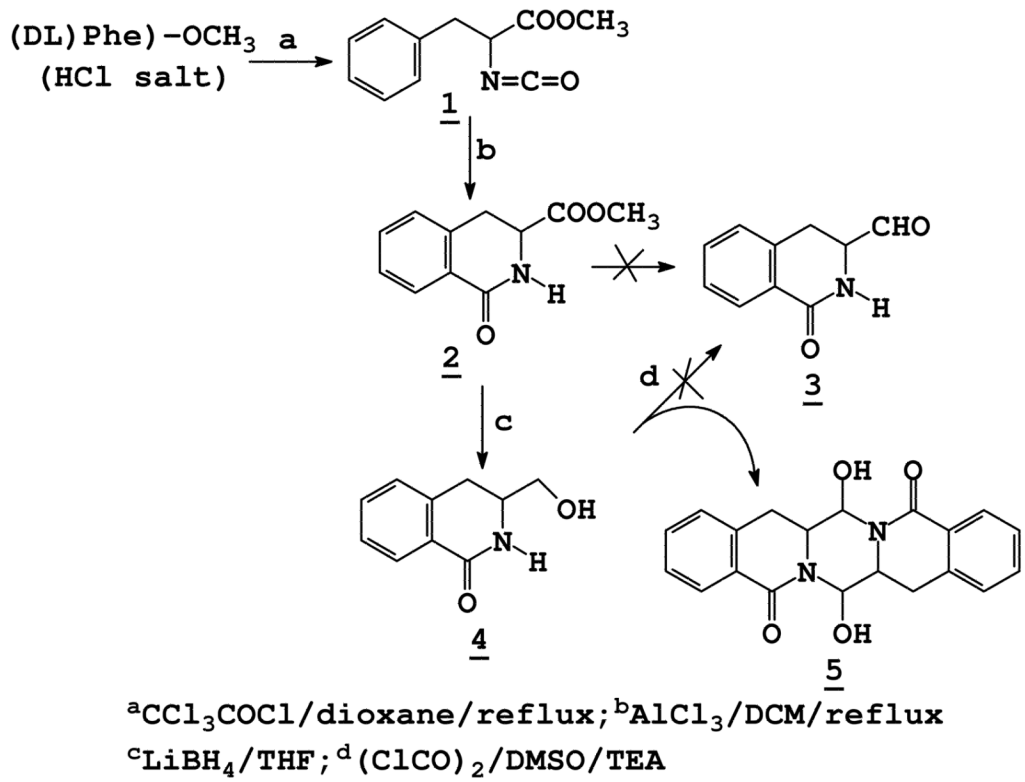

Scheme 1.

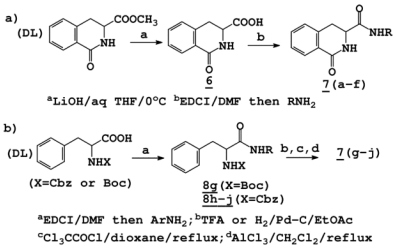

Scheme 2.

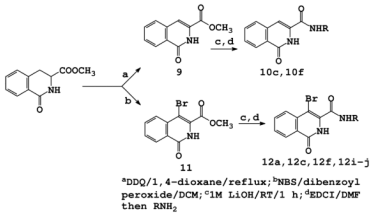

Scheme 3.

Table 1

Amine inputs

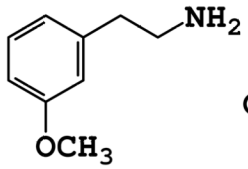 (7a/12a)	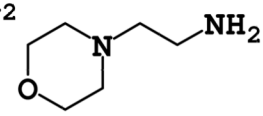 (7b)	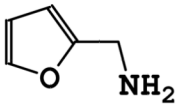 (7c/10c/12c)	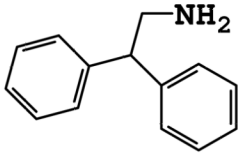 (7d)
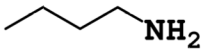 (7e)	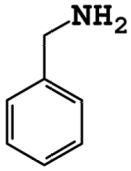 (7f/10f/12f)	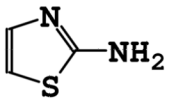 (7g)	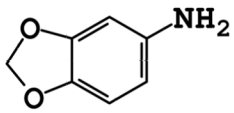 (7h)
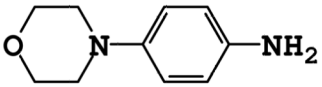 (7i/12i)	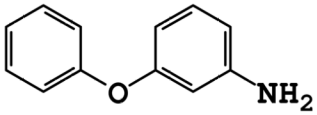 (7j/12j)		